Available online at www.sciencedirect.com
ScienceDirect
International Journal of Impact Engineering 35 (2008) 109–118
INTERNATIONAL JOURNAL OF IMPACT ENGINEERING
www.elsevier.com/locate/ijimpeng

A universal throw model and its applications

M.M. van der Voort[a,*], J.C.A.M. van Doormaal[a], E.K. Verolme[a], J. Weerheijm[a,b]

[a]TNO Defence, Security and Safety, P.O. Box 45, 2280 AA Rijswijk, The Netherlands
[b]Faculty of Civil Engineering and Geosciences, Delft University of Technology, The Netherlands

Received 28 April 2006; received in revised form 7 November 2006; accepted 8 January 2007
Available online 9 February 2007

Abstract

A deterministic model has been developed that describes the throw of debris or fragments from a source with an arbitrary geometry and for arbitrary initial conditions. The initial conditions are defined by the distributions of mass, launch velocity and launch direction. The item density in an exposed area, i.e. the number of impacting debris or fragments per unit of area, has been expressed analytically in terms of these initial conditions. While existing models make use of the Monte Carlo technique, the present model uses the source function theorem, an underlying mathematical relation between the debris density and the initial distributions. This gives fundamental insight in the phenomenon of throw, and dramatically reduces the required number of trajectory calculations.

The model has been formulated for four basic source geometries: a point source, a vertical cylinder, a horizontal cylinder, and a vertical plane. In combination with trajectory calculations the item density can be quantified. As an illustration of the model, analytical results are presented and compared for the vertical plane and the vertical cylinder geometry under simplified assumptions.

If uncertainties exist in the initial conditions, the model can be used to investigate these initial conditions based on experimental data. This has been illustrated on the basis of a trial with 5 ton of ammunition stacked in an ISO container. In this case the model has been successfully applied to determine the debris launch angle and velocity distribution, by means of backward calculations. If, on the other hand, sufficient information on the initial conditions is available, the model can be used as an effect model in risk assessment methods, or for the requirements on protective measures. The model can be used to predict safety distances based on any desired criterion.

Keywords: Debris; Fragments; Throw; Impact; Risk assessment

1. Introduction

The throw of debris and fragments is often the most dominant effect in explosion events. In case of deliberate explosions like those of ammunition shells, fragment throw determines the weapon effectiveness. In case of accidental explosions, like those in ammunition magazines and industrial explosions, the throw of debris plays an important role in the explosion hazard and consequently the required safety distances. As a result, the understanding and quantification of throw is of practical importance.

The initial conditions for throw are defined by the distributions of the mass, launch velocity and launch direction. These conditions are determined by a broad range of complex physical phenomena. Examples are the fragmentation process in case of (stacks of) ammunition shells, the break-up process of concrete buildings, and vessel rupture which is typical for industrial explosions. In general, the failure process is determined by the explosion load on the structure in relation to its strength. This process results in distributions of mass and launch direction. The subsequent acceleration by the expanding reaction products largely determines the distribution of launch velocities. This is accompanied by pressure relief as a result of the increasing vent area between the accelerating items.

These initial distributions are the required input for throw models. Most existing throw models make use of a Monte Carlo technique. Predefined distributions are sampled to obtain the initial conditions for a large number of trajectory calculations. The calculations result in a collection of impact locations in the field. An example of such a model is MUDEMIMP, a module within the

*Corresponding author. Tel.: +31 15 284 3462; fax: +31 15 284 3991.
E-mail address: martijn.vandervoort@tno.nl (M.M. van der Voort).

0734-743X/$ - see front matter © 2007 Elsevier Ltd. All rights reserved.
doi:10.1016/j.ijimpeng.2007.01.004

DISPRE code [1,2,3] for debris hazard prediction of ammunition magazines. A similar approach is taken with SPLIT-X [4], an expert system for the design of fragmentation warheads [5]. Another approach has been taken by Birnbaum [6] and Glanville [7], where debris dispersion from an ammunition magazine is simulated with the hydro code ANSYS AUTODYN [8].

The aim of the present study is to present the concept of a universal throw model, and its applications. The basis is the source function theorem, an underlying mathematical relation between the item density and the initial distributions [9,10]. The theorem is described in Section 2, together with the application to four basic geometries. In Section 3 analytical results are presented and compared for the vertical plane and the vertical cylinder geometry under simplified assumptions. Guidance on realistic initial distributions for a variety of explosion types is given in Section 4. In Section 5 the point source geometry is used to simulate a trial with 5 ton of ammunition stacked in an ISO container. The consequences of throw are discussed in Section 6, and conclusions are drawn in Section 7.

2. The source function theorem

2.1. Definition of the problem

A source area is defined which contains N items that will participate in the throw. The items obey a mass distribution which is discretized in K mass classes with populations N_k ($k = 1,\ldots,K$):

$$N = \sum_{k=1}^{K} N_k. \tag{1}$$

The average mass within each mass class is denoted as m_k ($k = 1,\ldots,K$). The total mass M that participates in the throw can then be expressed as

$$M = \sum_{k=1}^{K} M_k = \sum_{k=1}^{K} N_k \cdot m_k. \tag{2}$$

The mass M is not necessarily equal to the total mass initially present at the source area. In case of weak explosions like small quantities of high explosives [11], and gas- and dust-explosions [12], often only partial break-up occurs.

It is assumed that every mass class has a specific initial velocity $u_{0,k}$ ($k = 1,\ldots,K$).

The initial throw direction is described by two **source** variables. The primary source variable s_1 determines the trajectory properties. Examples are the initial elevation angle, and the initial height. The secondary source variable s_2 does not influence the trajectory properties but does influence the distribution of items in the exposed area. Examples are the azimuthal angle (angle in the horizontal plane) or a position along the source. This is illustrated in Fig. 1.

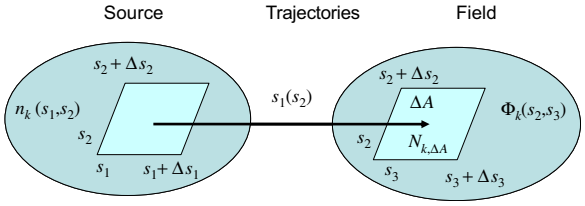

Fig. 1. Schematic overview of the source variables, the trajectories, and the field variables.

The distribution of items as a function of the source variables is defined by the source function $n_k(s_1,s_2)$ [9,10]. This source function is restricted by the 'conservation of items', expressed mathematically as

$$\iint_{\text{source}} n_k(s_1,s_2)\cdot J_{\text{source}}(s_1,s_2)\cdot \mathrm{d}s_1\cdot \mathrm{d}s_2 = N_k. \tag{3}$$

J_{source} is the 'Jacobian' of the source variables, and takes the curvature of the source variables into account. Integration has to be carried out over all relevant values of the source variables and results in the number of items in mass class k. If the source function fulfils this requirement it is called 'normalized'.

The exposed area is described by two *field* variables. The first is called the primary field variable s_3. Examples are the radial or linear distance to the source. The secondary field variable is equal to the secondary source variable s_2.

The source variables are coupled to the field variables by means of *trajectory* calculations, determined by gravity and drag [13]. Trajectory calculations are carried out for a range of values for the primary source variable s_1, and result in impact distances (s_3). These results are combined in a function $s_1(s_3)$, which can be obtained by interpolation. This function plays a key role in the determination of the item density.

The trajectory calculations also give the impact angles and impact velocities as output. From the item density and the impact angle, the number of hits per mass class on an object with given dimensions can be calculated. On the basis of the item mass and impact velocity, the consequences of throw, such as the probability of lethality or damage level, can be estimated. These steps are shown schematically in Table 1, and are described in Section 6.

2.2. Derivation of the source function theorem

The item density is defined as the number of impacting items per unit of area, and can be formulated mathematically as follows:

$$\Phi_k(s_2,s_3) = \lim_{\Delta A\to 0} \frac{N_{k,\Delta A}}{\Delta A}. \tag{4}$$

The element of area ΔA can be expressed in the field variables (from s_2 to $s_2+\Delta s_2$, and from s_3 to $s_3+\Delta s_3$):

$$\Delta A = J_{\text{field}}(s_2,s_3)\cdot \Delta s_2\cdot \Delta s_3. \tag{5}$$

Table 1
Schematic overview of the model

Source	Trajectories	Exposed area	Derived quantity 1	Derived quantity 2	Derived quantity 3
Source function (1/dim($s_1 \rightarrow s_2$))	$s_1 \rightarrow s_3$	Impact distances (m) s_3	Item density (#/m2) $\Phi_k(s_2,s_3)$	Number of hits N_{hits}	Consequences (Probability of lethality/damage level)
$n_k(s_1,s_2)$	$s_{1(s_3)}$				
Mass classes (kg) m_k	ds_1/ds_3	Impact angle (rad) $\alpha_{I,k}(s_3)$			
Velocity classes (m/s) $u_{o,k}$		Impact velocity (m/s) $u_{I,k}(s_3)$			

J_{field} is the 'Jacobian' of the field variables, and takes curvature of the field coordinates into account. When s_3 increases with s_1 the number of items impacting at ΔA can be written as

$$N_{k,\Delta A} = \int_{s_2}^{s_2+\Delta s_2} \int_{s_1(s_3)}^{s_1(s_3+\Delta s_3)} n_k(s_1', s_2') \cdot J_{source}(s_1', s_2') \cdot ds_1' \cdot ds_2'. \quad (6)$$

Eqs. (5) and (6) are inserted in the definition of the item density (4), and the limit is taken ($\Delta s_2 \rightarrow 0, \Delta s_3 \rightarrow 0$). This results in

$$\Phi_k(s_2, s_3) = n_k(s_1(s_3), s_2) \cdot \frac{J_{source}(s_1(s_3), s_2)}{J_{field}(s_2, s_3)} \cdot \frac{ds_1}{ds_3}. \quad (7)$$

The item density scales with the source function, the ratio of the 'source Jacobian' and the 'field Jacobian', and the first derivative of the primary source variable with respect to the primary field variable.

2.3. Application to four basic geometries

Eq. (7) has been applied to four basic geometries, which are defined in Table 2 together with some notes on the applications.

For a specific case one has to identify the relevant source geometry and the primary source variable, i.e. the main distribution variable for the throw. In the case of high explosives in ammunition magazines, impact distances are typically very large in relation to the magazine dimensions. In this case, the magazine can be considered as a point source with the elevation angle as the primary source variable. In the case of throw from a cylindrical silo wall due to a severe dust explosion, impact distances are comparable to the silo dimensions. In this case, the height along the silo wall should be chosen as the primary source variable, and the silo has to be modeled as a linear source (vertical cylinder).

The results for the four basic geometries are tabulated in Table 3. In the fourth column the item density is expressed in its most general form. Up to this point no assumptions have been made with respect to the source function.

If the elevation angle α is the primary source variable, the function $\alpha(r)$ or $\alpha(x)$ is not single-valued [9]. This is caused by the fact that in general there are two launch angles that result in the same impact distance. Fig. 2 illustrates the contributions from low launch angles ($\alpha_{low}(r)$) and high launch angles ($\alpha_{high}(r)$). In the case of an ammunition magazine debris throw from walls is determined by the low angle branch, while for roof debris it is determined by the high angle branch.

In the derivation of Eq. (7) it is assumed that s_3 increases with s_1. This requirement is fulfilled for the low angle debris (i.e. $d\alpha_{low}/dr > 0$). The opposite holds for high angle debris (i.e. $d\alpha_{high}/dr < 0$). As a result, for high angle contributions a minus sign has to be added to the equations for the item density in Table 3.

3. Homogeneous throw from a vertical plane and a vertical cylinder

When the source function is independent of the source variables, the throw is called 'homogeneous', and the source function is equal to a constant. The value of this constant follows directly from the 'conservation of items' (3). Results for this constant and the item density for this case are given in the fifth and sixth column of Table 3.

In this paragraph the model is illustrated with the simplified situation of homogeneous throw from a vertical plane and from a vertical cylinder. The focus is on a specific mass class 'k' with mass m_k and initial velocity $u_{0,k}$. It is assumed that m_k is sufficiently large, and $u_{0,k}$ is sufficiently small, so the drag force in the trajectory calculations can be neglected. In that case, the equations of motion can be solved analytically.

This is typically the case for debris throw due to a dust explosion in a reinforced concrete silo [12]. As an example Fig. 3 shows the situation after a series of dust explosions in a grain facility in Blaye (France) [14].

For the two basic geometries mentioned, a rather simple expression for the item density can be obtained. For a vertical cylinder with diameter D and height H the following result is obtained:

$$\Phi_k(r) = \frac{N_k \cdot g}{2 \cdot \pi \cdot H \cdot u_{0,k}^2} \cdot \left(1 - \frac{D}{2 \cdot r}\right), \quad (8)$$

Table 2
Definition of the four basic geometries and notes on the application

Source geometry	Primary source variable s_1 Secondary source/field variable s_2 Primary field variable s_3	Illustration	Application
Point source (spherical)	Elevation angle (α) Azimuthal angle (β) Radial distance (r)	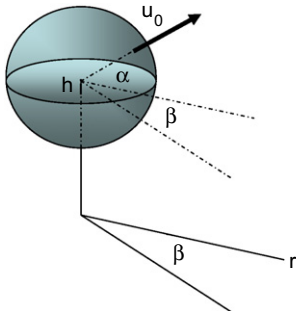	*Requirement* - Impact distances ≫ source dimension *Examples* - Ammunition shell - Ammunition storage (magagine, stack) - Industrial storage (building, vessel)
Linear source (vertical cylinder)	Initial height (h) Azimuthal angle (β) Radial distance (r)	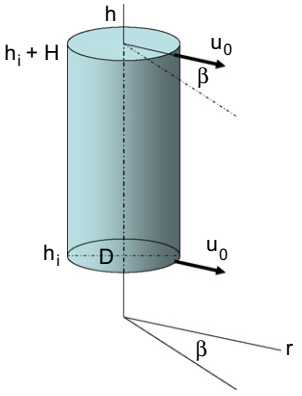	*Examples* - Vertical ammunition shell (close-in) - Industrial storage (silo building, vertical vessel)
Linear source (horizontal cylinder)	Elevation angle (α) Position (y) Linear distance (x)	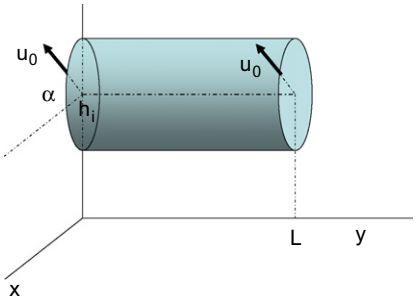	*Examples* - Horizontal ammunition shell (close-in) - Industrial storage (cylindrical roof, horizontal vessel)
Area source (vertical plane)	Initial height (h) Position (y) Linear distance (x)	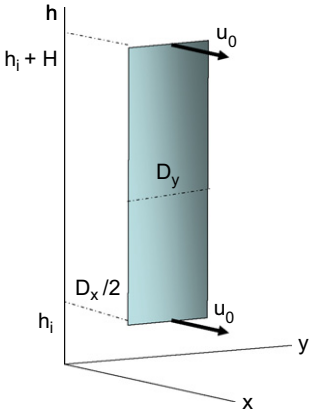	*Examples* - Ammunition magazine (close-in) - Industrial storage (silo building)

Table 3
The item density for the four basic geometries

Source geometry	Source Jacobian $J_{source}(s_1(s_3),s_2)$	Field Jacobian $J_{field}(s_2,s_3)$	Item density (general) $\Phi_k(s_2,s_3)$	Source function = homogenous (constant) = C_k	Item density (homogeneous) $\Phi_k(s_3)$
Point source (spherical)	$\cos(\alpha(r))$	r	$\frac{n_k(\alpha(r),\beta)\ \cos(\alpha(r))}{r}\ \frac{d\alpha}{dr}$	$\frac{N_k}{4\cdot\pi}$	$\frac{C_k\ \cos(\alpha(r))}{r}\ \frac{d\alpha}{dr}$
Linear source (vertical cylinder)	1	r	$\frac{n_k(h(r),\beta)}{r}\ \frac{dh}{dr}$	$\frac{N_k}{2\cdot\pi\cdot H}$	$\frac{C_k}{r}\ \frac{dh}{dr}$
Linear source (horizontal cylinder)	1	1	$n_k(\alpha(x),y)\cdot\frac{d\alpha}{dx}$	$\frac{N_k}{2\cdot\pi\cdot L}$	$C_k\cdot\frac{d\alpha}{dx}$
Area source (vertical plane)	1	1	$n_k(h(x),y)\cdot\frac{dh}{dx}$	$\frac{N_k}{D_y\cdot H}$	$C_k\ \frac{dh}{dx}$

Results are tabulated for a general source function (4th column), and for a homogeneous source function (6th column).

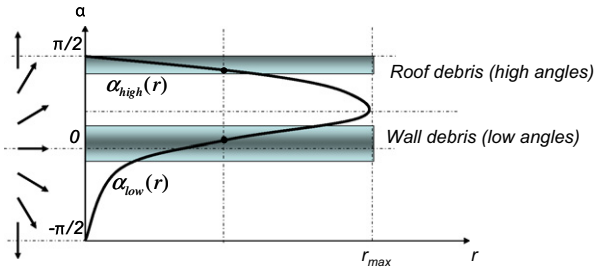

Fig. 2. Illustration of low and high angle contributions. The black curve represents the launch angle as a function of impact distance. The shaded areas indicate the relevant launch angles for wall and roof debris from an ammunition magazine.

Fig. 3. The Blaye accident (1997). After a series of dust explosions a large number of silo cells were totally destroyed.

with $r(h_i)\leqslant r\leqslant r(h_i+H)$, and

$$r(h)=\frac{D}{2}+u_{0,k}\cdot\sqrt{\frac{2\cdot h}{g}}.$$

This relation describes a ring-shaped throw pattern (Fig. 4) with an item density that slowly increases with distance (Fig. 5).

For a vertical plane with width D_y, and height H the following result is obtained:

$$\Phi_k(x)=\frac{N_k\cdot g}{D_y\cdot H\cdot u_{0,k}^2}\cdot\left(x-\frac{D_x}{2}\right), \tag{9}$$

with $x(h_i)\leqslant x\leqslant x(h_i+H)$, and $0yD_y$, and

$$x(h)=\frac{D_x}{2}+u_{0,k}\cdot\sqrt{\frac{2\cdot h}{g}}.$$

This relation describes a throw pattern with a rectangular shape located in front of the vertical plane (Fig. 4), with an item density that increases linearly with distance (Fig. 5).

The item density has been compared for the vertical cylinder and a composition of four vertical planes. In both cases an initial height h_i of 5 m and a wall height H of 40 m was chosen. In Fig. 5 the debris density has been scaled with the total number of items N_k. Results are shown for three different initial velocities.

From Fig. 5 it can be seen that the item density for the vertical cylinder is generally much smaller than that from the vertical planes, since the same number of items is spread over a larger area. While item distances increase with initial velocity, the item density decreases. The width of the throw pattern increases with initial velocity.

4. Realistic initial distributions

The quality of the model predictions is largely determined by the quality of the initial distributions. The simplified assumption of homogeneous throw, made in the previous paragraph, is in most practical situations not valid. In general, the distributions of mass, launch velocity and launch direction can be determined from experimental data or from numerical calculations. For a number of specific explosion types, the determination of the initial distributions is discussed.

For bare quantities of high explosives in ammunition magazines empirical relations for the distributions have been derived within the Klotz Group [15–21]. Those relations are based on debris pick-up data from a collection of large-scale trials, and depend on loading density and wall thickness. The cumulative debris mass distribution was found to decay exponentially with debris mass. The initial debris velocity also decreases with debris mass around a typical velocity; the debris launch velocity (DLV). This relation has been based on backward calculations. The launch angle distribution was found to be a rather sharp Gaussian distribution centered around a direction close to the wall normal

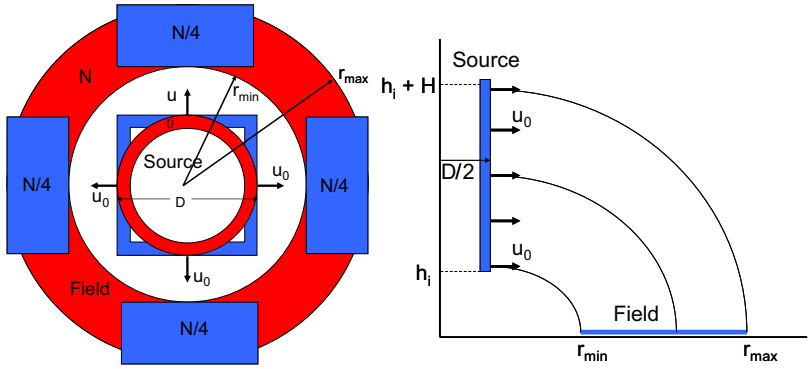

Fig. 4. Throw pattern from a vertical cylinder (red) and a composition of four vertical planes (blue). Top view (left) and side view (right).

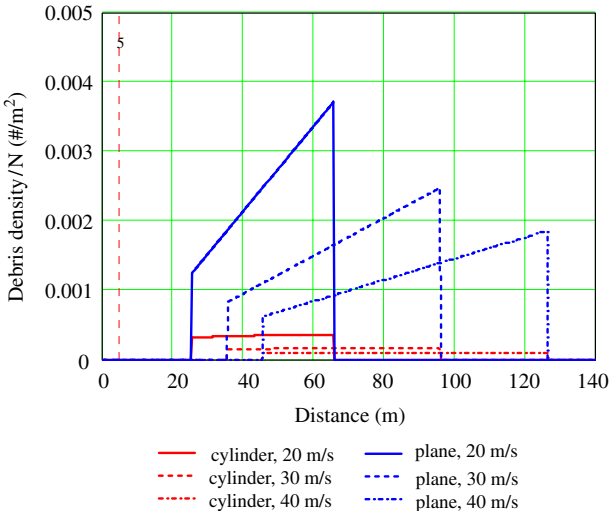

Fig. 5. Comparison of throw from a vertical cylinder and a composition of four vertical planes, both with an initial height h_i of 5 m, and a wall height H of 40 m. The diameter of the vertical cylinder and the width of the vertical planes equals 10 m. Scaled debris density versus distance.

direction. The addition of the new Sci Pan 3 trial to the database was recently reported [10]. The relations are currently being implemented in a software code, the KG-Engineering Tool [16].

For single ammunition shells a large amount of information is available on the initial distributions. As a first order approximation the Gurney formula can be used for the initial velocity and the Mott distribution for the fragment mass [22–24]. More detailed information can be found in so called JMEM (Joint Munitions Effectiveness Manual) data [25]. With codes such as SPLIT-X [4], the initial distributions can be obtained for a shell with an arbitrary shape [5]. The source function is altered by the shell impact angle and impact velocity which can be determined by codes such as PRODAS V3 (projectile design and analysis system) [26]. For ammunition shells in storage (stacks) the amount of information is limited. The current model has been used to analyze the initial conditions for a stack of 5 ton of ammunition which is reported in Section 5.

For industrial explosions such as bursting pressure vessels, internal gas explosions, runaway reactions, and BLEVE's (boiling liquid expanding vapor explosions) guidance can be found in the PGS02 [27], referred to as the 'Yellow Book'. In this reference a number of methods are discussed to estimate the number of fragments, their mass and initial velocity.

5. Application to the 5 ton trial

In this paragraph the application of the model to a trial with 5 ton of ammunition stacked in an ISO container is discussed. During this trial [28] 299 vertically placed 8'' M106C1 shells were detonated in a 20 ft ISO freight container. An illustration is shown in Fig. 6. The shells had a total equivalent charge weight of 5000 kg TNT.

After the detonation, all fragments were collected:

- with a mass larger than 100 g,
- at distances larger than 60 m from ground zero, and
- in half of the 36 radial sectors (of 10° each).

5.1. Mass classes

Assuming symmetry, the total number and mass of the collected fragments is multiplied by 2 to give 34.290 fragments with a total mass of 7.584 kg. This mass is equal to 32% of the total initial steel mass. The remaining 68% was either deposited within a distance of 60 m to ground zero or thrown out in fragments smaller than 100 g. In the current simulations the fragments are represented by the average mass of the collected fragments (0.23 kg), i.e. one mass class was defined.

5.2. Source function

On all four sides of the container, barricades were present, effectively blocking of fragments with launch angles up to typically 10–15° measured from ground level. Furthermore, 223 of the 299 shells were present in the bulk of the stack and their fragments are forced in upward direction. In the current simulation the stack is modeled as

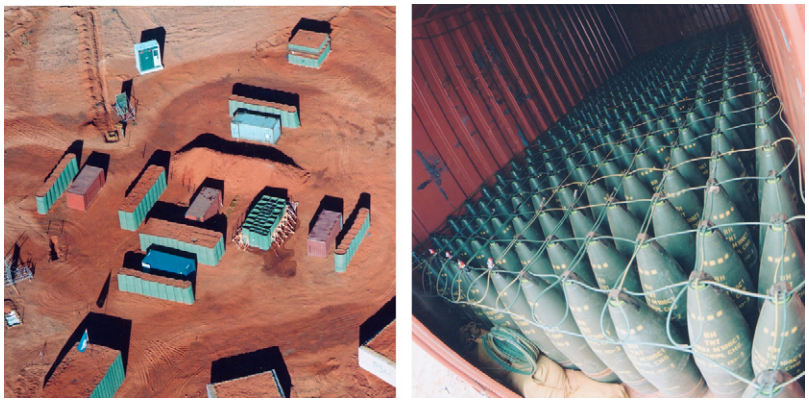

Fig. 6. An overview of the 5 ton trial. The 20 ft container with barricades (left). The internal of the 20 ft container with 299 M106C1 shells in vertical position (right).

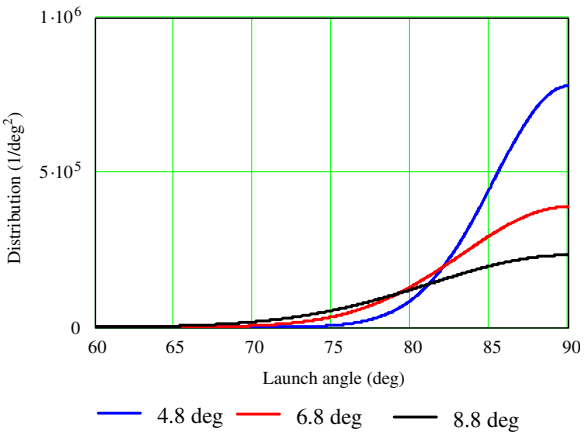

Fig. 7. The Gaussian distribution of fragments over the launch angles for three different standard deviations. Ninety degree corresponds to the upward direction.

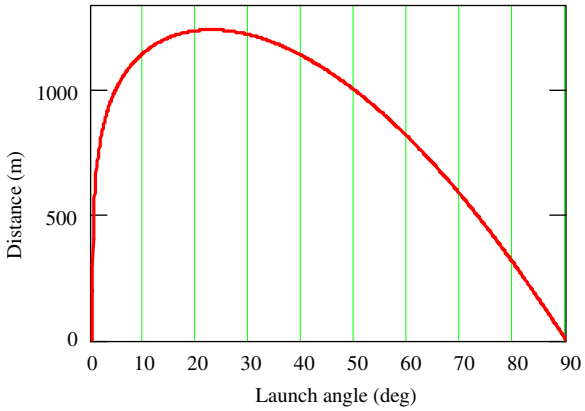

Fig. 8. Interpolated function of fragment distance versus launch angle for $m = 0.23$ kg and $u_0 = 1300$ m/s. Unbarricaded situation.

a point source with a Gaussian distribution of fragments over the launch angles. The distribution is assumed to be independent of the azimuthal angle. The average direction of fragments is upwards and the standard deviation has been varied. The normalized source function has been plotted in Fig. 7 for three standard deviations.

5.3. Velocity

For a single M106C1 shell, an initial fragment velocity of 942 m/s is reported [24]. For multiple closely stacked shells, the initial velocity of the leading fragments increases rapidly with the number of shells and reaches a maximum of approximately 2 times the initial 'single shell' velocity (~1900 m/s) for more than about 10 shells.

A Gurney analysis has been carried out with respect to the complete stack. In this analysis the stack is modeled as a 'flat sandwich' geometry [22]. An initial fragment velocity of 1760 m/s is obtained, which has to be interpreted as an average velocity. Experimental investigations confirm the occurrence of such high velocities [29], but also show a strong dependency on the launch angle. According to these investigations the velocity in the more relevant upward (nose) direction appears to be significantly lower in magnitude (~700 m/s for single shells and ~1300 m/s for stacks). In the current simulations the initial velocity has been varied.

5.4. Trajectory calculations

A number of 180 trajectory calculations have been carried out for launch angles from the horizontal (0°) to the vertical direction (90°). The shape of the fragments is assumed to be cubical, and a Mach number dependent drag coefficient based on experimental data [30,31] is used. In Fig. 8, the result for the fragment distance versus the launch angle is shown for an initial velocity of 1300 m/s. The curve shows a maximum at a launch angle of about 20°, which is a typical value for high velocity fragments. Note that for the geometry of the 5 ton test, only launch angles close to 90° are relevant.

5.5. Results

The resulting fragment density has been plotted together with the experimental result in Fig. 9. The red curve

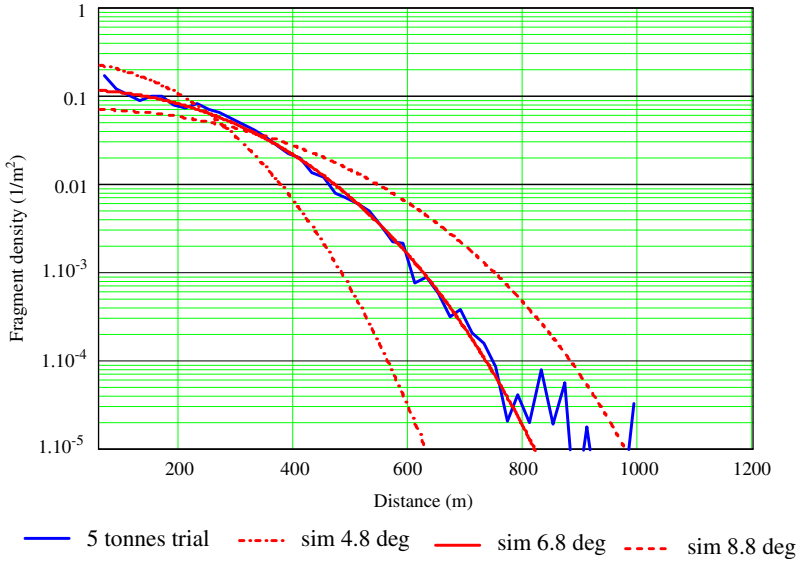

Fig. 9. Fragment density for the 5 ton trial. Experimental result (blue) and results from the simulations for $m = 0.23$ kg and $u_0 = 1300$ m/s with three standard deviations (red curves).

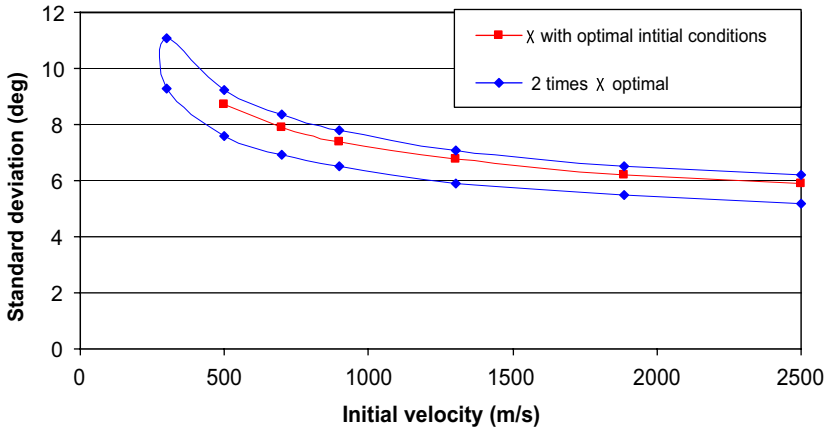

Fig. 10. The combinations of the initial fragment velocity (m/s), and the launch angle standard deviation (degree) that reproduce the 5 ton trial fragment density equally well (red). A contour representing the initial conditions resulting in 2 times the optimal χ is also displayed (blue).

(standard deviation 6.8°) shows excellent agreement with the experimental results up to 800 m. The small deviations above this distance are believed to be caused by some individual 'low angle' fragments that accidentally passed the barricades. The results for the other two standard deviations are shown to illustrate the large sensitivity to this parameter.

The quality of the model prediction has been determined with the quantity χ, which is related to ratio of the difference between simulation and experiment, and the measurement error:

$$\chi^2 = \frac{1}{N_{\text{data}}} \cdot \sum_{i=1}^{N_{\text{data}}} \frac{(\Phi_{\text{sim},i} - \Phi_{\text{exp},i})^2}{\Delta\Phi^2_{\text{exp},i}}, \tag{10}$$

with $\Phi_{\text{sim},i}$ the simulated fragment density at location i, $\Phi_{\text{exp},i}$ the measured fragment density at location i, $\Delta\Phi_{\text{exp},i}$ the measurement error at location i, and N_{data} the number of measurement locations.

The measurement error has contributions from debris pick up (estimated as 10%), and from the discretization of distances. Many combinations of the initial fragment velocity and the launch angle standard deviation, result in predictions with an optimal and equal value for χ. This is caused by the equivalence between a small initial velocity and a broad distribution, and a large initial velocity and a sharp distribution. In Fig. 10 these combinations are plotted with a red line. For high velocities the required standard deviation approaches a limit value in the order of 6°. For an initial velocity smaller then 300 m/s it is not possible to reach the largest observed fragment distances. The required standard deviation has a value between 6° and 7° for the more realistic values for the initial velocities (1300–1900 m/s). Fig. 10 also shows a contour representing

a value of 2 times the optimal value for χ. The model offers the opportunity to derive the most probable initial conditions based on experimental pick-up data.

6. The number of hits and the consequences

The total item density can be determined by addition of the contributions from the different mass classes (dependency on s_2 and s_3 is omitted from this point onwards):

$$\Phi = \sum_{k=1}^{K} \Phi_k.$$

However, in the evaluation of the consequences the different mass classes have to be treated separately. The number of hits due to mass class k on a certain object, can be calculated from the item density and the impact angle. The object is defined by a horizontal area A and a vertical area S, as illustrated in Fig. 11. The vertical area generates a 'shadow area' A_k:

$$A'_k = \frac{S}{\tan \alpha_{I,k}},$$

with $\alpha_{I,k}$ the impact angle, which depends on the mass class k.

As a result the number of hits can be formulated as

$$N_{\text{hits},k} = \Phi_k \cdot (A + A'_k).$$

It is assumed here that the item density is constant within areas A and A_k', and that trajectories have a downward direction at heights below the object height. This might be violated close to the source.

The total number of hits can be determined by the contributions from the different mass classes:

$$N_{\text{hits}} = \sum_{k=1}^{K} N_{\text{hits},k}.$$

The consequences of throw can be determined from the number of hits on an object for the different mass classes and their impact velocities. PGS01 [32] reports relations for the probability of lethality and damage level, based on the item mass and impact velocity. With this information, the consequences can be calculated at any location in the field.

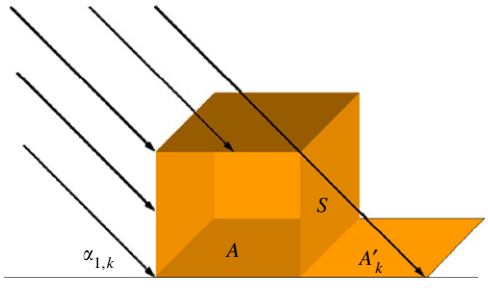

Fig. 11. Illustration of the 'shadow' area A'.

7. Discussion and conclusion

A universal throw model has been presented, and its applications have been discussed. The basis of the model is the source function theorem, a mathematical relation between the item density and the distributions of mass, launch velocity and launch direction. The theorem gives fundamental insight in the phenomenon of throw.

The model can be applied under the condition that only one source variable (the primary source variable) influences the trajectories. For example, in the case of a point source, the impact distances are determined only by the launch angle but not by the azimuthal angle. Under this condition the required number of trajectory calculations can be dramatically reduced when compared to the established Monte Carlo approach.

The model gives the item density as a continuous function of the field variables. This is an important advantage, especially at locations with small values of the item density. With a Monte Carlo approach, these small values can only be obtained with a very large amount of simulations.

The quality of the model predictions is largely determined by the quality of the initial distributions. If uncertainties exist in the initial conditions, the model can be used to investigate these initial conditions based on experimental data. This has been illustrated on the basis of a trial with 5 ton of ammunition stacked in an ISO container. In this case the model has been successfully applied to determine the debris launch angle and velocity distribution, by means of backward calculations.

There are some sources of error related to idealizations in the model. The first is determined by the translation of a construction to an idealized geometry. When an ammunition magazine wall is represented by a point source, reliable predictions of the debris density can only be expected at large ratios of distance versus magazine dimensions.

Furthermore, it is assumed that the initial velocity does not vary with the primary source variable, and that the initial velocity is constant within a mass class. The last assumption can be expected to be valid by dividing the items over a sufficient amount of mass classes. For debris throw from ammunition magazines the validity of these assumptions is under investigation within the Klotz Group [16].

If sufficient information on the initial conditions is available, the model can be used as an effect model in risk assessment methods, or for the requirements on protective measures. The model can be used to predict safety distances based on any desired criterion. An example is the IBD (inhabited building distance) which is defined as the distance above which the probability of lethality drops below 1% [23].

References

[1] Huang LCP. Theory and computer program for the multiple debris missile impact simulation (MUDEMIMP). Naval facilities engineer-

ing command, Naval Civil Engineering Laboratory, program no. Y0995-01-003-331, June 1984.
[2] Bowles MP. Practical use of the building debris hazard prediction model, DISPRE. Presented at the explosive safety seminar 1992 (DDESB).
[3] Bowles MP, Oswald CJ. Earth covered ammunition storage magazines, quantity-distance model, DISPRE2. Presented at the explosive safety seminar 1994 (DDESB).
[4] Rottenkolber E. SPLIT-X V5, An expert system for the design of fragmentation warheads. User manual, CONDAT GmbH, Scheyern-Fernhag, 2002.
[5] Rottenkolber E, Arnold W. A generalization of the Gurney formalism to three dimensions. 21st International symposium on ballistics, Adelaide, Australia, 19–23 April 2004.
[6] Birnbaum NK, Fairlie GE, Quan X. Coupled fluid–structure analysis of high explosive detonations in Masonry structures. Presented at the explosive safety seminar 2000 (DDESB).
[7] Glanville JP, Thayer RG, Hoing CA, Barnes IM. Masonry cube structure benchmark tests—hydrocode simulations. Presented at the explosive safety seminar 2006 (DDESB).
[8] AUTODYN-2D & 3D. User documentation, century dynamics, 2006.
[9] Van der Voort MM. The development of a physical model for the ballistics and deposition of fragments and debris. TNO report PML 2004-A59, Rijswijk, August 2004.
[10] van der Voort MM, Doormaal JCAM, Verolme EK, Weerheijm J. Analysis of the Sci Pan 3 debris throw data using the Klotz Group approach. Presented at the explosive safety seminar 2006 (DDESB).
[11] Verolme EK, et al. Quantity-distance relations for small quantities net explosive weight. TNO report TNO-DV2 2005 A051, Rijswijk, February 2006.
[12] Van der Voort MM, Klein AJJ, de Maaijer M, van den Berg AC, Deursen JR, Versloot NHA. A quantitative risk assessment tool for the external safety of industrial plants with a dust explosion hazard. TNO defence security and safety. Presented at the international symposium on hazards prevention and mitigation of industrial explosions (ISHPMIE), Halifax, Canada, 27 August–1 September 2006. p. 161–75.
[13] McCoy RL. Modern exterior ballistics: the launch and flight dynamics of symmetric projectiles, USA.
[14] Masson F. Explosion of a grain silo, BLAYE (France), summary report, INERIS, 1998.
[15] Van Doormaal JCAM, van der Voort MM, Verolme EK, Weerheijm J. Design of KG-Engineering Tool for debris throw prediction. TNO report TNO-DV2 2005 C112, Rijswijk, January 2006.
[16] van Doormaal JCAM, Weerheijm J, Klotz Group Engineering Tool for debris launch prediction. Presented at the explosive safety seminar 2006 (DDESB).
[17] van Doormaal JCAM, van den Berg AC, Weerheijm J. Theoretical and numerical support of the debris launch velocity. TNO Prins Maurits Laboratory, presented at the explosive safety seminar 2002 (DDESB).
[18] Weerheijm J, Doormaal JCAM, Gürke G, Lim HS. The break-up of ammunition magazines, failure mechanisms and debris distribution. TNO Prins Maurits Laboratory, presented at the explosive safety seminar 2002 (DDESB).
[19] Kummer P. Break-up of magazine walls due to explosions, debris launch angle, TM 201-03, 5 February 2005.
[20] Dörr A. Experimental investigation of the debris launch velocity from internally overloaded concrete structures. Final report DLV5 2003, Efringen-Kirchen, report I-73/03, December 2003.
[21] Gürke G. Experimental investigation of the debris launch velocity from internally overloaded concrete structures. Final report DLV3-2000, Efringen-Kirchen, report E 06/01, August 2001.
[22] Meyers MA. Dynamic behavior of materials. New York: Wiley; 1994.
[23] AASTP-1 (Allied Ammunition Storage and Transport Publication 1). Manual of NATO safety principles for the storage of military ammunition and explosives, May 1992.
[24] Methodologies for calculating primary fragment characteristics (TP 16). Department of Defense Explosives Safety Board, Alexandria, VA, 1 December 2003.
[25] MEM/AS. Target vulnerability, book 3 of 4 table 7-IX-8. Building mean areas of effectiveness (MAE)—structural damage, 61A1-AA-3-1 NAVAIR 00-130-ASR-1.
[26] PRODAS V3. Arrow Tech Associates, 1233 Shelburne Road, Suite South Burlington, VT 05403.
[27] Methods for the calculations of physical effects. Publicatiereeks Gevaarlijke Stoffen 2 (PGS 02). Ministerie van VROM, November 2005.
[28] Heemskerk AH. Evaluation of risk-NL regarding fragment/debris distribution. Review summary, TNO report PML 2004-A64.
[29] Kummer P. Explosion effects from ammunition in transit. Bienz, Kummer & Partner Ltd, Zollikerberg/Switzerland. Presentation at NATO AC/ 326 risk analysis workshop, Huntsville, AL/USA, April 2004.
[30] Dunn Jr DJ, Porter WR. Air drag measurements of fragments (U). Memorandum report no. 915, August 1955. Aberdeen Proving Ground, MD: Ballistic Research Laboratory.
[31] Engineering design handbook. Elements of terminal ballistics. Part one, introduction, kill mechanisms and vulnerability (U). AMCP 706-160, November 1962.
[32] Methods for the determination of possible damage to people and goods. Publicatiereeks Gevaarlijke Stoffen 1 (PGS 01). Ministerie van VROM, March 2005 [Dutch].